

EFFECT OF FIBRILLATION ON THE ABILITY OF CELLULOSE FIBERS TO SUPPRESS THE AGGREGATION OF QUINACRIDONE

YASUKO SAITO,* NAOYA HONTAMA,** YUKI TANAKA** and TAKASHI ENDO*

**Research Institute for Sustainable Chemistry, National Institute of Advanced Industrial Science and Technology (AIST), 3-11-32 Kagamiyama, Higashi-Hiroshima, Hiroshima 739-0046, Japan*

***Sanyo Color Works, Ltd., 81 Nobusue, Himeji, Hyogo 670-0966, Japan*

✉ *Corresponding author: Y. Saito, saitou.y4@aist.go.jp*

Received July 15, 2022

Quinacridone is a red–violet pigment often used as a coloring agent. However, the aggregation of quinacridone needs to be resolved to avoid undesirable color changes. Cellulose nanofibers are a potential candidate for novel pigment dispersants, due to their ability to inhibit aggregation. In this study, the effect of the degree of fibrillation of cellulose fibers on their performance as dispersants was investigated. Four types of highly fibrillated cellulose particles (HFCEPs) were prepared using a disk mill and a high-pressure homogenizer. The degree of fibrillation was evaluated using specific surface area measurements, scanning electron microscopy, and gravitational sedimentation analysis. Fibrillation of cellulose was found to increase its adsorption capacity toward quinacridone. Even partly fibrillated celluloses successfully inhibited the aggregation of quinacridone. Color measurements of the quinacridone–cellulose suspensions indicated that, although fibrillation of cellulose improves the chroma of the suspensions, excess fibrillation causes a decrease in the chroma.

Keywords: cellulose nanofiber, fibrillation, organic pigment, quinacridone, suppression of aggregation

INTRODUCTION

Organic pigments are coloring agents used to impart various hues to materials. They are insoluble in common solvents, owing to their strong tendency to aggregate. Post synthesis, the organic pigment molecules assemble through intermolecular interactions to form crystals. These small assemblies are called primary particles. The primary particles further flocculate to form larger clusters called secondary particles. The size of primary and secondary particles influences the color strength, rheological characteristics, and opacity of the pigments.^{1–4} Therefore, controlling the aggregation behavior of organic pigments can enhance their performance. Blocks and/or grafted polymers are often used to disperse pigments in aqueous media. Some polymer dispersants consist of hydrophilic and hydrophobic moieties. The hydrophobic segments are adsorbed onto the pigment particles and cover their surface, whereas, the hydrophilic segments present in the medium prevent the aggregation of pigment particles by steric hindrance and ionic repulsion.⁵

In our previous study, we reported that cellulose nanofibers (CNFs) could be a potential pigment dispersant for quinacridone, a common red–violet organic pigment.^{6,7} The mechanism by which CNFs prevent the aggregation of quinacridone appears to be different from that of polymer dispersants. Quinacridone easily aggregates through NH \cdots O hydrogen bonding and π – π stacking.^{8,9} Upon addition to an aqueous suspension of quinacridone, the CNFs adsorbed quinacridone primary particles after only a few minutes of sonication. NMR and IR spectroscopies indicated that cellulose and quinacridone might interact through hydrogen bonding between the glucose residue of cellulose and NH group of quinacridone, as well as the CH– π interaction between the CH group of cellulose and aromatic moiety of quinacridone. These interactions can help CNFs achieve an excellent quinacridone-adsorption capacity as the quinacridone adsorption onto CNF is preferred to the primary particle aggregation.

In contrast, commercially available cellulose powder does not adsorb quinacridone or inhibit its aggregation. This would be because the specific surface area of cellulose powder is considerably smaller than that of CNFs, so that the sites of cellulose powder are too small to adsorb quinacridone. However, the effect of different morphologies of CNFs on their dispersing properties of quinacridone pigments has not been sufficiently ascertained. In this study, we investigated the influence of the degree of cellulose fibrillation on their ability to inhibit the aggregation of quinacridone. A series of

highly fibrillated cellulose particles (HFCEs) with different degrees of fibrillation were prepared from cotton powder. Cotton powder was chosen as the raw material because it mostly comprises cellulose, and therefore will help to exclude the influence of other components. The degree of fibrillation of the HFCEs was evaluated based on their specific surface area, surface morphology, and sedimentation behavior. To elucidate the dispersion process of the quinacridone particles, the effect of sonication time on quinacridone aggregation was also investigated.

EXPERIMENTAL

Materials

Quinacridone powder (γ -form) was pulverized by salt milling to reduce the average diameter of the primary particles to 60 nm. Milled quinacridone was washed with water and used without drying to inhibit further aggregation. Quinacridone dispersion with a concentration of 5 wt% was prepared using distilled water. Cotton powder (40–100 mesh, Toyo Roshi Kaisha, Ltd., Tokyo, Japan) was used as cellulose powder; the cellulose powder comprised 99.51 wt% cellulose, 0.48 wt% Klason lignin, and 0.01 wt% ash. Distilled water was used to prepare suspensions of quinacridone, cellulose, and their mixtures. Other chemicals were purchased from FUJIFILM Wako Pure Chemical Corporation (Osaka, Japan) and were used as received.

Preparation of HFCEs with different degrees of fibrillation

The cellulose powder was immersed overnight in water; the concentration of the cellulose suspension was adjusted to 5 wt%. The dispersion was then treated with a disk mill (MKCA6-2, Masuko Sangyo Co., Ltd., Saitama, Japan) to fibrillate the cellulose powder. Two ceramic nonporous disks were set to rotate at 1800 rpm. Fibrillation treatment was repeated while gradually narrowing the distance between the two disks. A portion of the suspension was set aside during three different stages of fibrillation, and were labeled as HFCEs (i), (ii) and (iii), in decreasing order of their degrees of fibrillation. Cellulose powder and HFCE (iii) were from the same lot as used in our previous study.⁷

A portion of HFCE (iii) was diluted to a concentration of 1 wt% with distilled water. This dispersion was further fibrillated using a high-pressure homogenizer (MASSCOMIZER MMX-L200-D10, Masuko Sangyo Co., Ltd., Saitama, Japan) at a pressure of approximately 200 MPa. The obtained fibrillated fiber was labeled as HFCE (iv).

Characterization of cellulose powder and HFCEs

The sedimentation behaviors of the cellulose powder and HFCEs in water were evaluated using the gravitational sedimentation method. Each dispersion was diluted to a concentration of 0.1 wt%. The dispersions were placed in a test tube with 24 mm diameter, and filled up to a height of approximately 50 mm. The light transmission of the dispersions was measured every 1 min, for 30 min at room temperature using a stability analyzer (Turbiscan TOWER, Formulation Inc., Toulouse, France). The wavelength of the light source (λ_{air}) used was 850 nm.

A portion of each cellulose dispersion was subjected to solvent exchange with *tert*-butyl alcohol and freeze-dried. The specific surface area of the freeze-dried cellulose powder and HFCEs was determined from the Brunauer–Emmett–Teller (BET) plots of their nitrogen adsorption isotherms using a BELSORP-max (BEL Japan, Inc., Tokyo, Japan) system. The morphology of the freeze-dried HFCEs was observed using field-emission scanning electron microscopy (FE-SEM S-4800, Hitachi High-Technologies Co., Tokyo, Japan); an accelerating voltage of 1.0 kV was used for the measurements. The samples were prepared by placing the HFCEs on a conductive tape and vapor depositing osmium onto them using an osmium coater (Neoc-Pro, Meiwafoods Co., Ltd., Tokyo, Japan).

Adsorption of quinacridone on cellulose powder and HFCEs

The suspensions of cellulose powder and HFCEs (i)–(iii) were diluted to a concentration of 2 wt% and were added to 10 g of quinacridone suspension (2 wt%) in varying ratios; the quinacridone-to-cellulose weight ratios were 1:0, 2:1, 1:1, 1:2, 1:4, 1:9, and 1:19. Distilled water was added to each mixture until their mass reached 200 g, so that the quinacridone concentration became 0.1 wt%. Later, each mixture was sonicated for 1 min using an ultrasonic homogenizer (US-150T, NIHONSEIKI KAISHA Ltd., Tokyo, Japan), equipped with a 20 mm diameter probe tip at 19.5 kHz. Out of each of the 200 g of dispersions, 50 g was set aside for the measurements. The residual dispersions were sonicated for 9 min.

HFCE (iv) was collected by centrifugation and re-dispersed to prepare a 2 wt% aqueous suspension. The mixtures of quinacridone and HFCE (iv) were prepared in the same manner as the other quinacridone–cellulose mixtures, except that here the total amount of each dispersion was 100 g.

Evaluation of adsorption capacity of fibrillated celluloses

The amount of quinacridone adsorbed by different batches of the HFCPs were compared using the same method described in our previous report.⁷ Several tens of milliliters of quinacridone–cellulose dispersions were filtered through a nylon mesh N-NO.508S (pore size: 20 μm , AS ONE CORPORATION, Osaka, Japan) and then a nylon membrane NY1004700 (pore size: 10 μm , Merck KGaA, Darmstadt, Germany) to separate the non-adsorbed quinacridone from the mixed dispersions. The cellulose fibers that were smaller than the filter mesh could pass through it, and were removed from the filtrate by decantation. Absorption spectra of the obtained supernatants were recorded using a UV–vis spectrometer V-670 (JASCO Corporation, Tokyo, Japan) to evaluate the amount of non-adsorbed quinacridone. The supernatants were diluted using distilled water before measurements, if their absorbance at approximately 555 nm, derived from quinacridone, was higher than 1.73. The absorbance of the original supernatant was calculated assuming that Lambert–Beer’s law holds. The absorption of 0.001–0.01 wt% quinacridone aqueous dispersions was also measured for comparison.

SEM of the quinacridone–cellulose complexes

The aggregation behavior of quinacridone particles in the presence and absence of HFCPs was evaluated using SEM of freeze-dried samples, which was performed in the same manner as described earlier.

Color measurements

The quinacridone–cellulose aqueous dispersions, in which the concentration of quinacridone was 0.1 wt%, were subjected to color measurements. The color properties (L^* , a^* , b^*) were determined from the reflection spectra, recorded from 360 to 740 nm using a CM-5 spectrophotometer (KONICA MINOLTA, Inc., Tokyo, Japan). L^* , a^* , and b^* represent lightness, the green (-)/red (+) axis, and the blue (-)/yellow (+) axis respectively. A D65 illuminant was used for the measurements. The specular component included (SCI) mode, and the observer at 2° was selected. The diameter of the cell was 30 mm. The chroma value C^* was calculated using Equation 1:¹⁰

$$C^* = \sqrt{((a^*)^2 + (b^*)^2)} \quad (1)$$

All measurements were performed five times for each sample and the average values were calculated.

RESULTS AND DISCUSSION

Characterization of fibrillated cellulose

Cellulose powder was fibrillated by disk milling to obtain disintegrated HFCPs (i)–(iii). A portion of HFCP (iii) was further fibrillated using a high-pressure homogenizer. The specific surface areas of the freeze-dried cellulose powder and HFCPs (i)–(iv) are listed in Table 1. The specific surface areas of the celluloses increased from 8.5 cm^2/g (cellulose powder) to 141.2 cm^2/g (HFCP (iii)). However, treating HFCP (iii) with a high-pressure homogenizer did not increase their specific surface area. SEM images demonstrated that disk milling the cellulose powder first partially fibrillated the ends and surfaces of the fibers. Subsequently, the repeated disk-milling treatments gradually peeled the fibers to produce nanofibers (Fig. 1). The diameters of cellulose fibers in HFCP (iii) were estimated to be 20–180 nm from the SEM micrograph.⁷ However, a few fibers were insufficiently fibrillated and remained several hundred nanometers in diameter. Although the diameter of HFCP (iv) was comparable to that of HFCP (iii), seldom fibers of the former had submicron diameters.

The sedimentation behavior of cellulose fibers in water depends on their size, morphology, and surface condition.^{11,12} The appropriate fiber size for sedimentation analysis differs according to the method used to settle the samples, such as gravity or centrifugal force. The gravitational sedimentation of CNFs reflects the degree of fibrillation, especially the difference between low- and medium-fibrillated CNFs.¹³ In this study, the gravitational sedimentation behavior of the HFCPs was evaluated using a stability analyzer. Figure 2 shows the change in light transmission of the aqueous cellulose suspensions (0.1 wt%) over time. When the fibers settle out, the concentration of HFCPs in the suspension varies with the height. This is reflected in the profile of the transmission light intensity. The horizontal axis in Figure 2 represents the distance from the bottom of the test tube to the surface of the suspension (Fig. 2f). Cellulose powder and HFCP (i) settled out and immediately reached a constant sedimentation rate (Figs. 2a and b). With an increase in fibrillation, the change in light transmission of the suspensions decreased. HFCP (ii) settled gently (Fig. 2c). The light transmission of HFCP (iii) remained constant during the measurement (Fig. 2d). The HFCP (iii) suspension was considered to be stable for 30 min. The light transmission of HFCP (iv) at 0 min was higher than that of HFCP (iii). This might be due to the absence of sub-micron fibers. Conversely, HFCP (iv) gradually

settled after 30 min (Fig. 2e). A rapid increase in the transmitted light around the top of the suspension suggested that a small amount of large aggregates in the suspension settled out.¹⁴

The results of the aforementioned analyses demonstrated that repeating the disk-mill process consistently reduced the diameter of the cellulose fibers, thereby increasing the specific surface area of the fibers. Notably, the gravitational behavior of HFCP (ii) was different from that of the cellulose powder, although the former was only partly fibrillated, as indicated by specific surface area analysis and SEM. This might be due to the fiber coarseness of HFCP (ii).¹³ The diameter and specific surface area of HFCP (iii) were in agreement with the characteristics of the CNFs. HFCP (iii) did not settle under the conditions of the sedimentation test in this study. Additional fibrillation using a high-pressure homogenizer did not change the specific surface area. However, this process reduced the number of fibers with large diameters, making the morphology of the fibers uniform. The sedimentation behavior indicated that HFCP (iv) was prone to re-aggregation. The size distribution of HFCP (iv) was assumed to be one of the reasons for its aggregation behavior, although further investigations, such as changes in molecular weight, are needed to confirm this.

Table 1
Specific surface areas of the cellulose powder and HFCPs

Sample	Specific surface area
	(S_{BET} , m^2/g)
Cellulose powder	8.5
HFCP (i)	14.4
HFCP (ii)	37.5
HFCP (iii)	141.2
HFCP (iv)	140.5

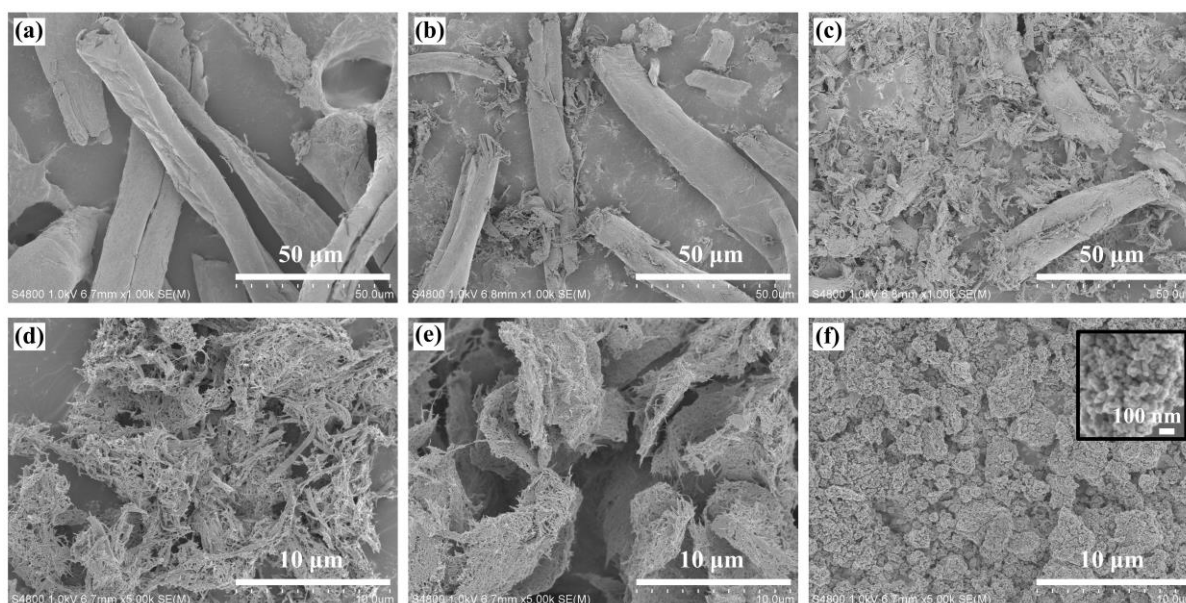


Figure 1: SEM images of (a) cellulose powder, HFCP (b) (i), (c) (ii), (d) (iii), (e) (iv), and (f) quinacridone particles

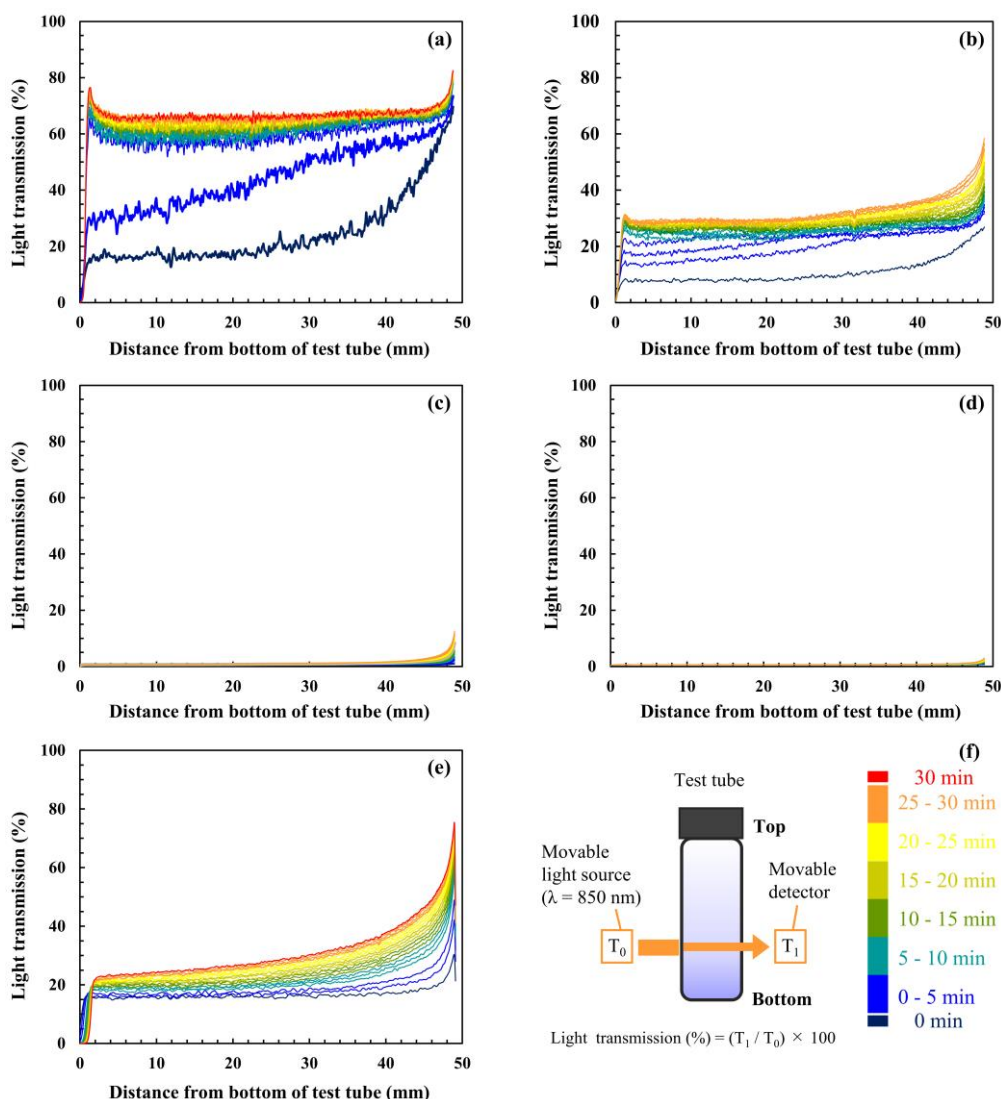


Figure 2: Sedimentation profiles of (a) cellulose powder, HFCP (b) (i), (c) (ii), (d) (iii), and (e) (iv); Measurement principle of stability analyzer is shown in (f)

Adsorption of quinacridone on HFCPs

Aqueous suspensions of quinacridone and HFCPs (i)–(iv) were mixed in a weight ratio of 2:1, 1:1, 1:2, 1:4, 1:9 and 1:19. The quinacridone concentration was adjusted to 0.1 wt%. The mixtures were shaken by hand and then subjected to ultrasonic treatment for 1 min. A series of quinacridone–cellulose powder suspensions was prepared in the same manner. To evaluate the adsorption capacity of each HFCP, we separated the quinacridone that was not adsorbed onto cellulose from the suspensions by filtration and decantation. However, we were unable to do this for the mixture with HFCP (iv), because many of the fibers passed through the filter. Thus, the quinacridone–HFCP (iv) mixture was not subjected to the adsorption test.

The UV–vis spectrum of the quinacridone aqueous suspension exhibited absorption peaks at 520 and 555 nm in the visible light region. The absorbance at 555 nm (A_{555}) was proportional to the concentration of quinacridone, at least in the concentration range 0.001–0.01 wt%; A_{555} varied from 0.18 to 1.73. The relationship between quinacridone concentration (0.001–0.01 wt%) and A_{555} was determined using Equation 2:

$$y = 175.42x \quad (2)$$

where symbols x and y represent quinacridone concentrations (wt%) and A_{555} , respectively. The R-squared value was 0.9998.

The absorbance of quinacridone in the UV–vis spectra of the supernatants obtained from the quinacridone–cellulose suspensions is plotted in Figure 3a. The spectra exhibited absorption peaks at

554–556 nm. When the absorbance was higher than 1.73, the supernatant was diluted, and the original absorbance was calculated according to Lambert–Beer’s law. The absorbance of the supernatants from the quinacridone–cellulose powder suspension was slightly lower than that of the 0.1 wt% quinacridone suspension. Furthermore, their absorbance remained almost constant, regardless of the weight ratio of cellulose powder. This result was consistent with that of our previous report.⁷ HFCP (i) exhibited similar results to that of cellulose powder. Using Equation 2, the quinacridone concentrations in the supernatant of quinacridone–cellulose powder and HFCP (i) (1:19, w/w) were calculated to be 0.092 and 0.082 wt%, respectively. This indicated that cellulose powder and HFCP (i) adsorbed less than 20% of the original amount of quinacridone particles, even when the amount of cellulose added was 19 times more than that of quinacridone. Conversely, A_{555} of quinacridone–HFCP supernatants (ii) and (iii) decreased substantially as the amount of cellulose increased. The A_{555} of the supernatant of quinacridone–HFCP (ii) (1:19, w/w) was 0.66 and that of quinacridone–HFCP (iii) (1:19, w/w) was 0.01. The quinacridone concentrations in the supernatant of quinacridone–HFCP (ii) and quinacridone–HFCP (iii) (1:19, w/w) were calculated to be 3.8×10^{-3} wt % and 6.9×10^{-5} wt%, respectively.

The quinacridone concentration of the supernatants and the total surface area of the added HFCPs were calculated from Equation 2 and Table 1, respectively, and are plotted in Figure 3b. This indicated that the adsorption capacity of the HFCPs improved with their surface area. Interestingly, HFCP (ii) adsorbed more quinacridone than the other HFCPs with the same surface area. We speculate that this is because partial fibrillation at the surface of the fibers may facilitate the adsorption of quinacridone.

SEM observation

Next, the morphology of quinacridone particles was observed using SEM. In the absence of additives, the primary particles of quinacridone (60 nm) aggregated to form secondary particles with a diameter of several micrometers (Fig. 1f). To investigate the effect of cellulose on the aggregation behavior of quinacridone, we performed SEM of the freeze-dried quinacridone–cellulose mixtures. Figure 4 shows the SEM images of the quinacridone–HFCP (iii) mixture. The micrograph of quinacridone–HFCP (iii) mixture (2:1, w/w) shows that the quinacridone primary particles were not dispersed. Some of them formed large secondary particles of the order of micrometers in diameter (Fig. 4a). In Figure 4b, the aggregates of quinacridone could be still observed, but the diameter of the secondary particles became smaller. When an amount of HFCP (iii) nine times that of quinacridone was added, the quinacridone primary particles were adsorbed on the CNFs and did not aggregate.

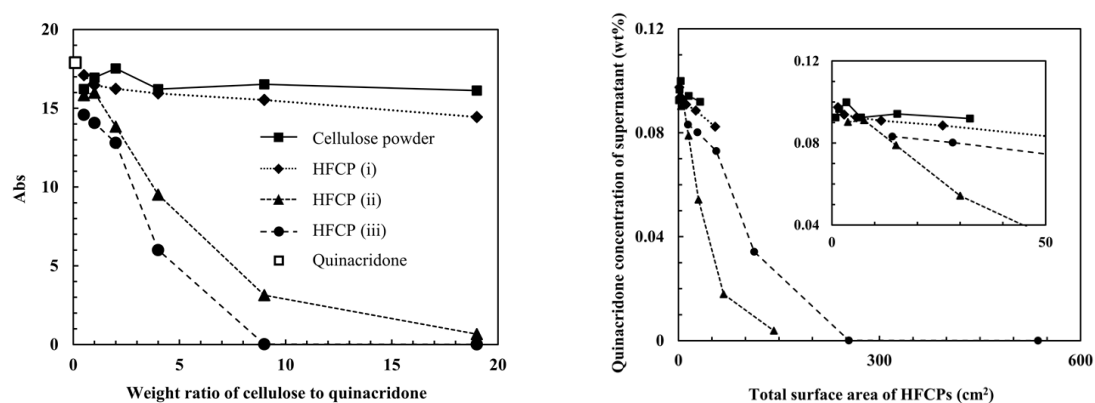


Figure 3: Evaluation of the adsorption capacity of HFCPs toward quinacridone. (a) Absorbance derived from quinacridone of the supernatant of quinacridone–cellulose suspensions after filtration and decantation (absorption peaks observed at 554–556 nm; hollow squares show the absorbance of the aqueous quinacridone suspension at 555 nm); (b) Relationship between the total surface area of the cellulose fibers and quinacridone wt% of the supernatant; inset picture shows a magnified version of the plot from 0 to 50 cm²

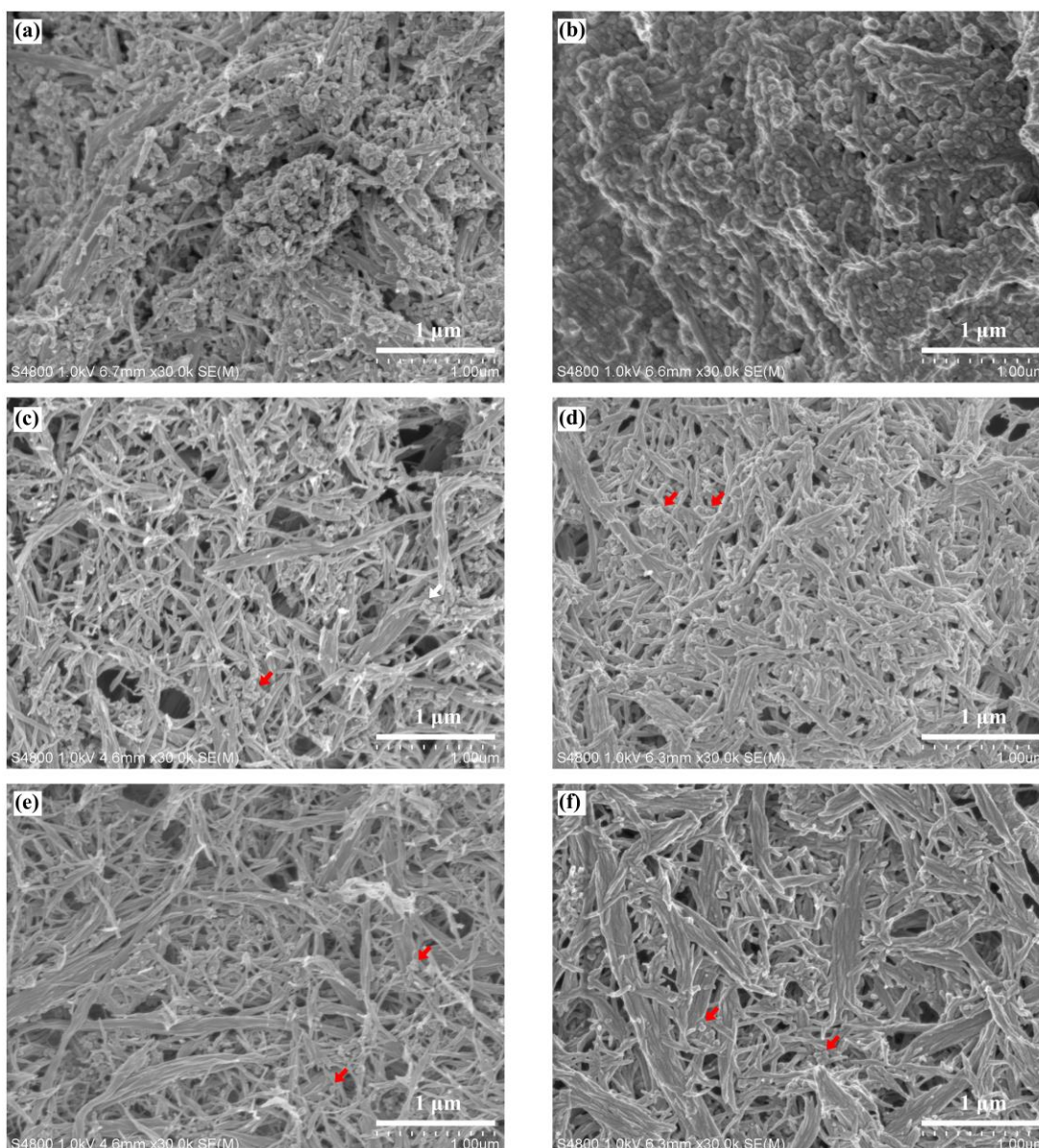


Figure 4: SEM images of mixtures of quinacridone and HFCP (iii), mixed in the ratios: (a) 2:1 (w/w), (b) 2:1 (w/w), (c) 1:4 (w/w), (d) 1:4 (w/w), (e) 1:9 (w/w), and (f) 1:9 (w/w). Mixtures (a), (c), and (e) were sonicated for 1 min and mixtures (b), (d), and (f) were sonicated for 10 min. Arrows show the quinacridone particles

We then compared the aggregation of quinacridone based on the differences in the HFCPs. Figure 5 shows the morphology of quinacridone–cellulose mixture (1:9, w/w). When quinacridone and cellulose powder were mixed, quinacridone aggregates with sizes of the order of micrometers were observed (Fig. 5a). In the case of the quinacridone–HFCP (i) mixture, the aggregates still formed, but their sizes were smaller than that of the aggregates of quinacridone–cellulose powder (Fig. 5b). The dispersion of quinacridone proceeded when processed with HFCP (ii) (Fig. 5c). The SEM image of quinacridone–HFCP (iv) (Fig. 5d) was similar to that of quinacridone–HFCP (iii), indicating that both HFCPs (iii) and (iv) might suppress the aggregation of quinacridone primary particles. The aggregation-inhibiting effect of the HFCPs on quinacridone seemed to be in agreement with their adsorption capacity for quinacridone.

Sonication is widely used to disperse insoluble solids in solvents. However, sonicating the aqueous dispersion of quinacridone did not remove the aggregation. This indicates that sonication without any dispersants might be insufficient to fracture the quinacridone aggregates. Figure 4 (b, d and f) shows the SEM images of quinacridone–HFCP (iii) mixtures (2:1, 1:4 and 1:9) after sonicating them for an additional 9 min. When quinacridone was mixed with a sufficient amount of HFCP (iii), the primary

particles of quinacridone remained dispersed after additional sonicating (Fig. 4d and e). In Figure 4b, the quinacridone secondary particles, which were observed in Figure 4a, disappeared, and quinacridone primary particles covered the surface of the cellulose fibers. This suggests that the quinacridone primary particles might be dispersed along the cellulose fibers.

Based on the aforementioned results, we proposed a mechanism to suppress the aggregation of quinacridone using cellulose (Fig. 6). When the HFCP was added to the quinacridone aqueous suspension, the secondary quinacridone particles were adsorbed onto the cellulose fibers. The adsorption was thought to be induced through intermolecular interactions, such as hydrogen bonding and CH- π interactions between cellulose and quinacridone.⁶ During subsequent sonication, the quinacridone primary particles might be peeled off from the surface of the secondary particles. This procedure was repeated to disperse the primary particles around the cellulose fibers. However, it should progress only when the intermolecular interactions between cellulose and quinacridone are larger than those between the quinacridone primary particles. Fibrillation of cellulose might have an effect on its quinacridone-adsorption capacity. For example, fibrillation of cellulose fibers by high-pressure homogenization has been reported to expose the hydrophobic (200) plane of the cellulose crystal, which originally existed inside the cellulose crystal, providing Janus-type amphiphilic cellulose nanofibrils.^{15,16} Quinacridone aromatic moieties are expected to interact with the cellulose hydrophobic plane through CH- π interactions. Therefore, the fibrillation of cellulose could facilitate the adsorption of quinacridone by increasing the number of cellulose molecules that interact with quinacridone molecules, albeit through weak intermolecular interactions, such as CH- π interactions.

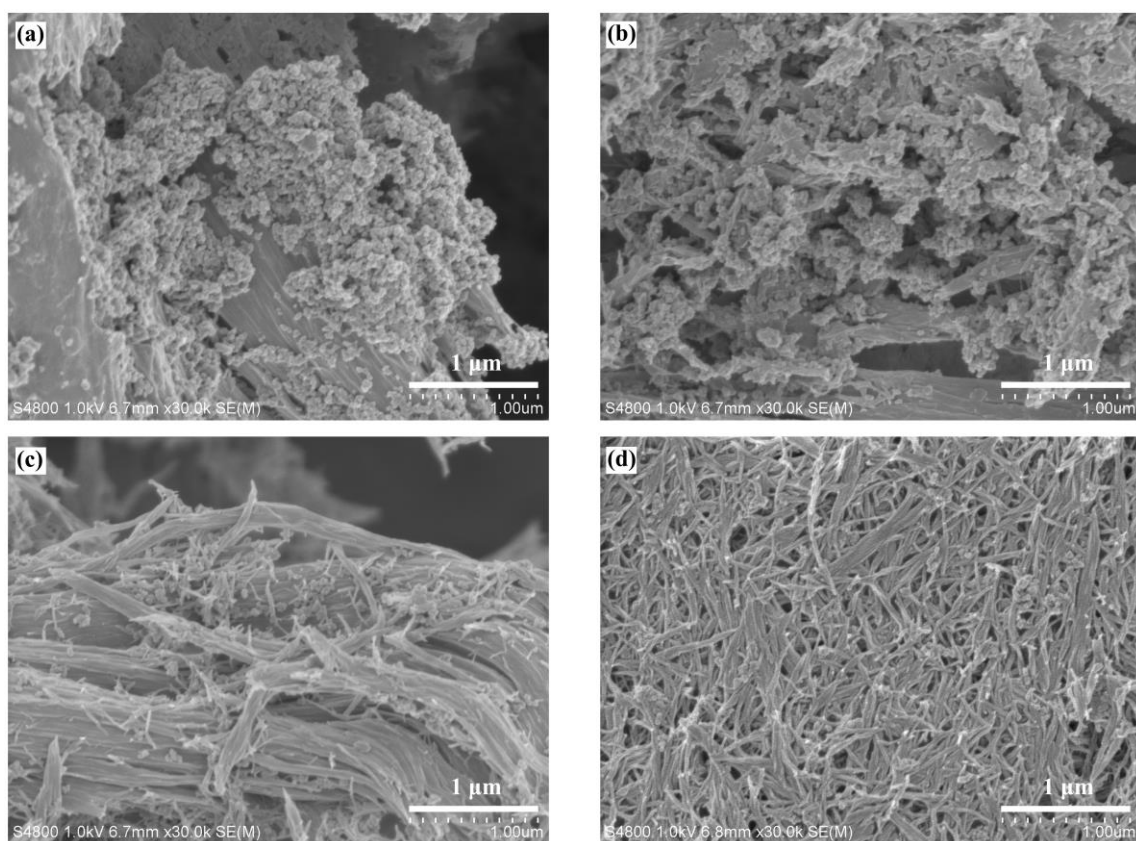


Figure 5: SEM images of quinacridone–cellulose mixtures with different fibrillation degrees of cellulose; (a) cellulose powder, (b) HFCP (i), (c) HFCP (ii), and (d) HFCP (iv); (the weight ratio of quinacridone and cellulose was 1:9)

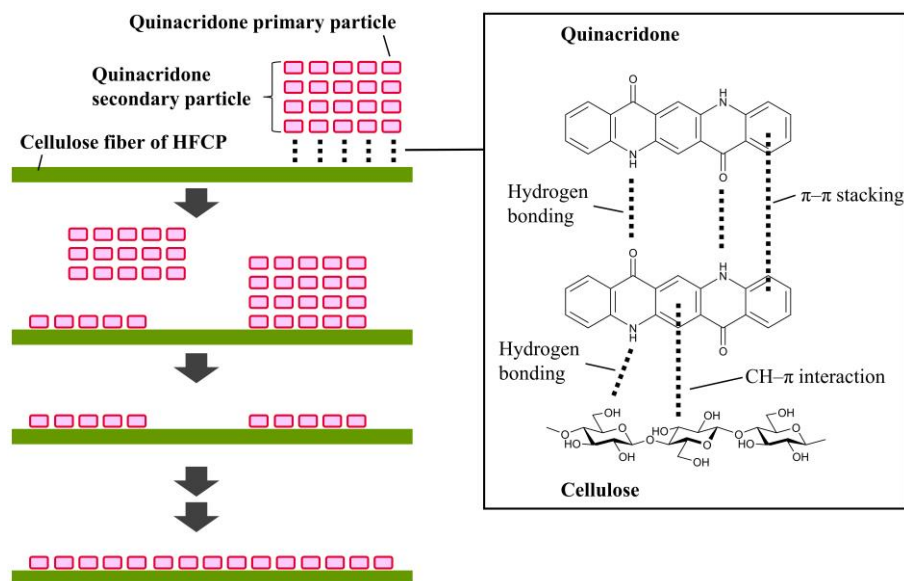


Figure 6: Schematic of the plausible mechanism of suppression of quinacridone aggregation by HFCPs

Color measurement

We then evaluated the colors of the quinacridone and quinacridone–cellulose suspensions. The concentration of quinacridone was adjusted to 0.1 wt% in all suspensions. The color parameters L^* , a^* , b^* , and C^* are shown in Figure 7. The values of L^* , a^* , and b^* of the 0.1 wt% quinacridone aqueous suspension were 34.18, 36.42, and 8.24, respectively, which were different from the previously reported values ($L^* = 20.99$, $a^* = 31.63$, $b^* = 4.38$).⁷ This inconsistency most likely stems from the difference in measurement conditions. The light path length through the suspension was ca. 10 mm in this study, whereas it was 4 mm in the previous work. Moreover, in this study, light was irradiated from the bottom of the cell without a white calibration plate on the other side of the cell, whereas in the previous study, light was irradiated from the side of the cell with a calibration plate on the other side of the cell.

Upon addition of the cellulose powder to the quinacridone aqueous suspension, the color parameters L^* and a^* increased, whereas parameter b^* remained almost constant, regardless of the amount of cellulose added. This observation was consistent with that of the previous report.⁷ Color parameters of the suspensions of quinacridone–HFCP (i) and (ii) exhibited similar shifts to that of the quinacridone–cellulose powder suspension. It should be noted, however, that the parameters L^* and a^* of quinacridone–HFCP (ii) were much higher than those of the quinacridone–cellulose powder suspension. As the weight ratio of HFCP (ii) increased from 2:1 to 1:19, L^* and a^* increased from 34.54 to 41.66, and from 37.12 to 51.11, respectively. When quinacridone was treated with HFCPs (iii) and (iv), the parameters L^* and a^* increased, whereas the parameter b^* decreased with an increase in the amount of cellulose. The color parameters L^* , a^* , and b^* of quinacridone–HFCP (iii) suspension (1:19, w/w) were 43.61, 53.28, and 6.06, respectively, and those of quinacridone–HFCP (iv) suspension (1:19, w/w) were 40.96, 48.30, and 4.37, respectively. According to our previous report, as the primary particles in the quinacridone aqueous suspension disperses, L^* and a^* increases, whereas b^* decreases.⁷ This indicates that HFCPs (iii) and (iv) inhibited the aggregation of quinacridone, resulting in a change in the color of the quinacridone aqueous suspension. However, considering that HFCP (ii) also suppressed the aggregation of quinacridone (Fig. 5), quinacridone aggregation alone is not sufficient to explain the difference in the color of the suspensions. The color parameters L^* and a^* of the quinacridone–cellulose mixtures, increased in the following order: HFCP (iv) < (ii) < (iii). In addition, the parameter b^* of the quinacridone–HFCP (ii) suspension (1:19, w/w) was the highest among all mixtures.

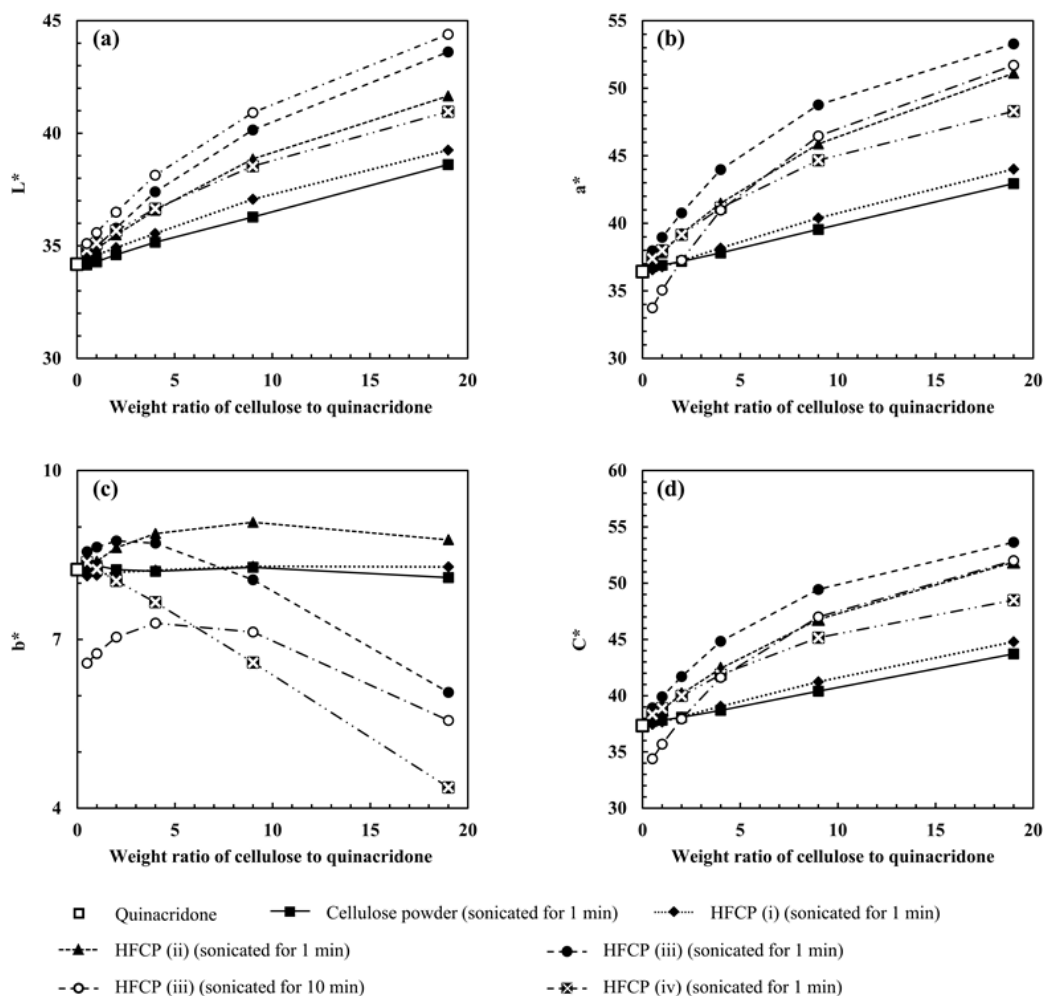


Figure 7: Effect of HFCPs on color parameters (a) L^* (lightness), (b) a^* (green (-)/red (+) axis), (c) b^* (blue (-)/yellow (+) axis), and (d) C^* (chroma)

As quinacridone is insoluble in water, the brilliance and hue of the suspension were affected not only by the selective absorption of visible light but also by its scattering.^{1,4} We, therefore, compared the reflectance spectra of the quinacridone–cellulose mixtures (1:9, w/w), quinacridone, and cellulose aqueous suspensions (Fig. 8). In the spectra of the quinacridone–cellulose powder (1:9, w/w) and quinacridone–HFCP (i) (1:9, w/w), the reflectance in the red region (640–740 nm) was higher than that of the quinacridone aqueous suspension. In the spectra of the quinacridone–HFCP (ii), quinacridone–HFCP (iii), and quinacridone–HFCP (iv) suspensions, the reflectance in the violet–blue region (360–460 nm), as well as the reflectance in the red region was greater than that of the quinacridone suspension. However, the reflectance of the aqueous suspension of HFCPs (ii) and (iii) did not show any clear peaks (Fig. 8b and c). The whole reflectance of HFCP suspensions increased with the weight ratio and the degree of fibrillation of the cellulose fiber, except for HFCP (iv). Surprisingly, the reflectance spectrum of the quinacridone–cellulose suspension was not simply the sum of those of the quinacridone and HFCP suspensions. Although further investigations are needed, we speculate that the surface topology of the HFCPs changes upon adsorbing quinacridone, resulting in a change in the light transmission, scattering, and refraction of the suspension.

Finally, the parameter C^* , which represents the chroma of the samples, was calculated from parameters a^* and b^* . C^* of the quinacridone aqueous suspension was 37.34 (Fig. 7d). C^* tended to increase with the addition of cellulose powder and HFCPs. For quinacridone–cellulose mixtures with a weight ratio of 1:19, C^* was found to decrease in the following order: HFCP (iii), (ii), (iv), (i), and cellulose powder. The C^* value of quinacridone–HFCP (iii) suspension (1:19) was 53.63, which was 1.4 times higher than that of the quinacridone aqueous suspension. These results indicate that fibrillation of cellulose fibers enhances their ability to increase the color strength of quinacridone.

However, when the degree of fibrillation of cellulose fibers rises above a certain level, the light reflectance of the quinacridone–cellulose suspension begins to decline, resulting in a decrease in their chroma. Upon further sonication of the quinacridone–HFCEP (iii) suspension, L^* increased, whereas a^* and b^* decreased (Figs. 7a–c). As a result, the chroma of the suspension declined (Fig. 7d). Therefore, one minute of sonication was sufficient to degrade the aggregation of quinacridone secondary particles and improve the color strength of the suspension.

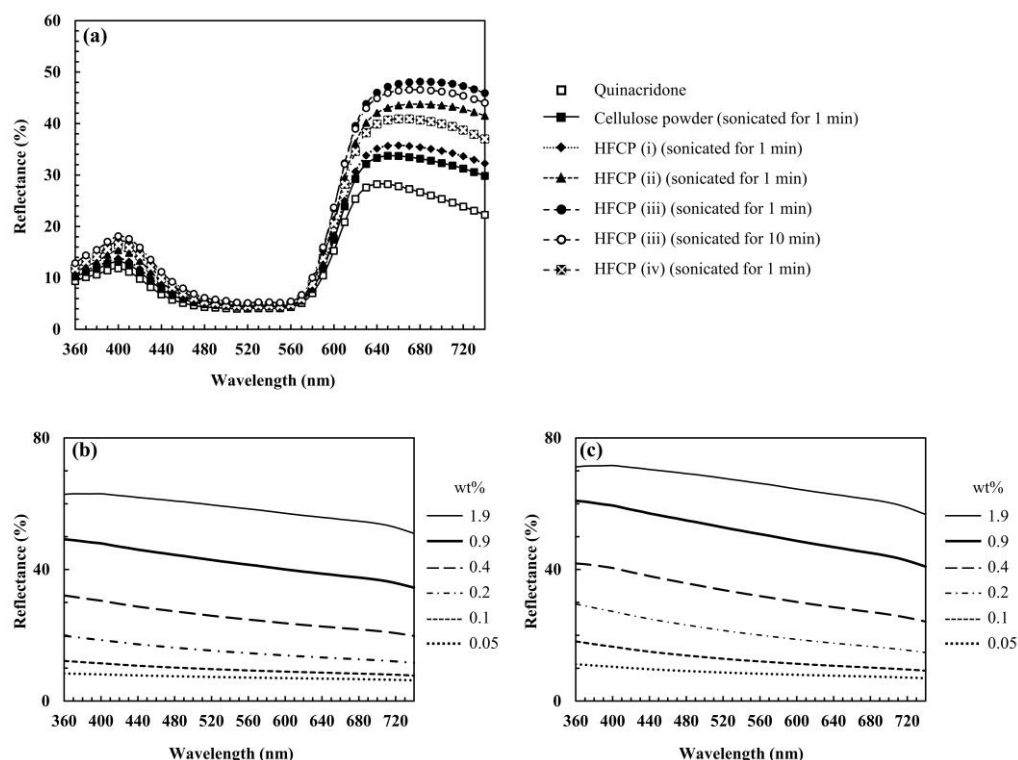


Figure 8: Reflectance spectra of (a) quinacridone suspension and quinacridone–cellulose suspensions (1:9, w/w), (b) HFCEP (ii) suspension, and (c) HFCEP (iii) suspension

CONCLUSION

We investigated the influence of the fibrillation of cellulose on the aggregation and color of quinacridone particles. Cellulose powder from cotton was used as raw material. HFCEPs with four different degrees of fibrillation were prepared by disk milling and subsequent high-pressure homogenization. Cellulose powder as such seldom adsorbed quinacridone and did not suppress its aggregation. However, as fibrillation increases, the capacity of the HFCEPs to adsorb quinacridone particles increases. SEM observations showed that HFCEPs, with a specific surface area above $37.5 \text{ m}^2/\text{g}$, suppressed the formation of quinacridone secondary particles. A comparison of the quinacridone–cellulose mixtures that were sonicated for 1 and 10 min indicated that the quinacridone primary particles might be adsorbed onto cellulose fibers and peeled off from the quinacridone secondary particles during sonication. The adsorption–desorption process may be repeated to disperse the primary particles separately. The fibrillation of cellulose fibers increases their adsorption capacity for quinacridone by increasing the number of adsorption sites. For example, if the hydrophobic (200) plane of cellulose crystals is exposed, $\text{CH}-\pi$ interactions between the CH group of cellulose and the aromatic moiety of quinacridone could be facilitated. The color parameters of the quinacridone–cellulose aqueous suspension were different from those of the quinacridone aqueous suspension, although the quinacridone concentration was the same. The chroma C^* tended to increase when HFCEPs with a high degree of fibrillation were used. We speculate that the difference in color parameters could be caused by several factors. First, the suppression of quinacridone aggregation might be related to the increase in the parameters L^* , a^* , and C^* , as well as the decrease in the parameter b^* . Second, the morphologies of the HFCEPs are thought to influence the light reflectance of the suspension. In addition, the change in the surface geometries of the HFCEPs upon adsorbing quinacridone might also affect the light scattering and light refraction of the quinacridone–cellulose

suspensions. In conclusion, fibrillation of cellulose fiber facilitated its performance as a dispersant of quinacridone, although excess fibrillation caused a decrease in the chroma of the quinacridone–cellulose aqueous suspensions.

ACKNOWLEDGEMENTS: We would like to thank Editage (www.editage.com) for English language editing.

REFERENCES

- ¹ Z. Hao and A. Iqbal, *Chem. Soc. Rev.*, **26**, 203 (1997), <https://doi.org/10.1039/cs9972600203>
- ² G. Skillas, N. Agashe, D. J. Kohls, J. Ilavsky, P. Jemian *et al.*, *J. Appl. Phys.*, **91**, 6120 (2002), <https://doi.org/10.1063/1.1466524>
- ³ H. Sis and M. Birinci, *Colloid. Surfaces A Physicochem. Eng. Asp.*, **455**, 58 (2014), <https://doi.org/10.1016/j.colsurfa.2014.04.042>
- ⁴ A. Mulderig, G. Beaucage, K. Vogtt, H. Jiang, Y. Jin *et al.*, *Langmuir*, **33**, 14029 (2017), <https://doi.org/10.1021/acs.langmuir.7b03033>
- ⁵ H. J. Spinelli, *Adv. Mater.*, **10**, 1215 (1998), [https://doi.org/10.1002/\(SICI\)1521-4095\(199810\)10:15<1215::AID-ADMA1215>3.0.CO;2-0](https://doi.org/10.1002/(SICI)1521-4095(199810)10:15<1215::AID-ADMA1215>3.0.CO;2-0)
- ⁶ Y. Saito, S. Iwamoto, N. Hontama, Y. Tanaka and T. Endo, *Cellulose*, **27**, 3153 (2020), <https://doi.org/10.1007/s10570-020-02987-0>
- ⁷ Y. Saito, S. Iwamoto, Y. Tanaka, N. Hontama and T. Endo, *Carbohydr. Polym.*, **255**, 117365 (2021), <https://doi.org/10.1016/j.carbpol.2020.117365>
- ⁸ M. Sytnyk, E. D. Głowacki, S. Yakunin, G. Voss, W. Schöfberger *et al.*, *J. Am. Chem. Soc.*, **136**, 16522 (2014), <https://doi.org/10.1021/ja5073965>
- ⁹ P. Chen, G. J. Liu, Y. Wang and S. X. A. Zhang, *RSC Adv.*, **6**, 25986 (2016), <https://doi.org/10.1039/c6ra01487a>
- ¹⁰ R. A. Viscarra Rossel, B. Minasny, P. Roudier and A. B. McBratney, *Geoderma*, **133**, 320 (2006), <https://doi.org/10.1016/j.geoderma.2005.07.017>
- ¹¹ T. T. T. Ho, K. Abe, T. Zimmermann and H. Yano, *Cellulose*, **22**, 421 (2015), <https://doi.org/10.1007/s10570-014-0518-6>
- ¹² N. Butchosa and Q. Zhou, *Cellulose*, **21**, 4349 (2014), <https://doi.org/10.1007/s10570-014-0452-7>
- ¹³ A. Kumagai, M. Adachi and T. Endo, *Japan Tappi J.*, **73**, 461 (2019), <https://doi.org/10.2524/jtappij.1901>
- ¹⁴ M. Mazloumi, L. J. Johnston and Z. J. Jakubek, *Cellulose*, **25**, 5751 (2018), <https://doi.org/10.1007/s10570-018-1961-6>
- ¹⁵ T. Tsuji, K. Tsuboi, S. Yokota, S. Tagawa and T. Kondo, *Biomacromolecules*, **22**, 620 (2021), <https://doi.org/10.1021/acs.biomac.0c01464>
- ¹⁶ G. Ishikawa, T. Tsuji, S. Tagawa and T. Kondo, *Macromolecules*, **54**, 9393 (2021), <https://doi.org/10.1021/acs.macromol.1c01163>